In vitro digestibility of gels from different starches: relationship between kinetic parameters and microstructure

Andrea ALEIXANDRE[a], Yaiza BENAVENT-GIL[a], R. MOREIRA[b], Cristina M. ROSELL[a]*

[a]Institute of Agrochemistry and Food Technology (IATA-CSIC). C/Agustin Escardino, 7. 46980-Paterna. Spain. (andrea.aleixandre@csic.es; yaizabenavent@gmail.com; crosell@iata.csic.es)

[b]Department of Chemical Engineering, Universidade de Santiago de Compostela, rúa Lope Gómez de Marzoa, Santiago de Compostela, E-15782, Spain. (ramon.moreira@usc.es)

*Corresponding author: Cristina M. Rosell, Institute of Agrochemistry and Food Technology (IATA-CSIC). C/Agustin Escardino, 7. 46980-Paterna. Spain. crosell@iata.csic.es

Abstract

Starch performance along digestion is becoming of utmost importance owing to the extensive presence of starch in foods and its association to the foods glycaemic index. However, scarce information exists on the relationship between the digestibility of starch gels and their microstructure. The aim of the study was to identify the rate and degree of digestion of starch gels from different botanical sources and the impact of gels microstructure with the *in vitro* starch digestibility (IVSD) by fitting the hydrolysis kinetics. Starch gels from cereals, tubers, and pulses were structurally analyzed and subjected to a standardized oro-gastrointestinal IVSD. The gel microstructure was significantly different among starches. Cereal gels had thinner walls than tuber and pulses gels, and this discrimination was not evident in the area of the gel cavities. Starches hydrolysis was well fitted to a first-order kinetics model, except for rice starch gel. Potato and chickpea gels showed the slowest digestion, and in the case of potato gel some starch remained undigested at the end of the digestion. The amylose content of gels was correlated with starch hydrolysis rate. Moreover, starch gels with thinner walls and/or bigger cavities seems to facilitate the enzyme action, and therefore, the starch digestibility.

Keywords: starch gel, *in vitro* digestion, first-order kinetics, cereals, pulses, tubers

1. Introduction

Starch is a polymeric carbohydrate present in cereals, tubers, and pulses, and the most important energy source in the human diet (Chambers, Byrne, & Frost, 2019). The chemical composition, structure and properties of starches depend on their biological origin (Jayakody & Hoover, 2008), which also determines the microstructure of the resulting gels, particularly regarding shapes and hole sizes (Garzon & Rosell, 2020).

The recent concern about the increase of diabetes prevalence, and its relationship with the consumption of starchy foods, has prompted much research on how to modulate starch hydrolysis and predict the glucose release and absorption following ingestion of starchy foods (Martinez, 2020). The starch digestion rate and absorption determine the postprandial metabolic response after meal ingestion (Goñi, Garcia-Alonso, & Saura-Calixto, 1997). Starch digestion starts in the oral cavity, by the action of the salivary α-amylase enzyme, and continues in the intestine, by the action of pancreatic α-amylase and α-glucosidase enzymes, after being subjected to the stomach conditions. Enzyme-based approach used in the *in vitro* digestion models offers an easier and cheaper alternative to *in vivo* methods (Butterworth, Warren, Grassby, Patel, & Ellis, 2012). Recently, the international COST INFOGEST network developed a standardized protocol for *in vitro* food digestion (Brodkorb, et al., 2019).

When starchy foods are cooked or baked, the starch granules gelatinize, representing more than 90% of the total consumed starch (Lineback & Wongsrikasem, 1980). Most of the enzymatic digestion studies focused their investigation on starch rich food or granular starches (Bustos, Vignola, Pérez, & León, 2017; Zhang, Ao, & Hamaker, 2006). In those studies different methods have been used to fit starch-enzyme digestion curves, like first-order kinetics (Goñi, et al., 1997), or Log of slope plots (LOS)

(Butterworth, et al., 2012). Among them, the first-order mathematical equation proposed by Goñi, et al. (1997) to fit starch hydrolysis curves ($C = C_\infty(1 - \exp(-kt))$) has been commonly applied to study the starchy food digestion (Chung, Lim, & Lim, 2006; Frei, Siddhuraju, & Becker, 2003; Segura & Rosell, 2011). Alternatively, first-order model involves two parameters related to the digestion equilibrium (equilibrium concentration, C_∞) and the digestion rate (kinetics constant, k). Nevertheless, in those studies, only some of them reported the hydrolysis of gels from starches using the INFOGEST oro-gastro-intestinal standardized method (Feltre, Almeida, Sato, Dacanal, & Hubinger, 2020; Lavoisier & Aguilera, 2019; Noda, et al., 2008). However, despite the applicability of this method to follow the impact of different compounds on digestion, to our best knowledge there is no information about the hydrolysis kinetics of starch gels. Therefore, we initially hypothesize that the oro-gastrointestinal standardized method could be applied to starch gels.

The main purpose of this study was to study the starch hydrolysis kinetics of different starch gels by applying the oro-gastrointestinal standardized method. The particular objectives included: (i) the characterization of the microstructure of starch gels, (ii) the analysis of *in vitro* oro-gastrointestinal digestion of gels and (iii) the experimental starch hydrolysis data fitting using a first-order kinetic-based model. For that purpose, different starches, three from cereals (wheat, corn, rice), two from pulses (green pea, chickpea), one from potato and other from cassava were selected. Although, cassava is a root tuber, not a tuber like potato, henceforth both starches will be grouped as tuber starches.

2. Materials and methods

2.1. Materials

The following starches were used: wheat starch (ADM Chamtor, Bazancourt, France), corn starch (Tate & Lyle PLC, London, United Kingdom), rice starch (Sigma Chemical, St. Louis, USA), potato starch (Tereos, Lille, France), cassava starch (local market), and green pea starch (*Pisum sativum*) (Esteve Santiago, Valladolid, Spain). Chickpea was purchased in the local market and used for starch isolation.

Type VI-B α-amylase from porcine pancreas (EC 3.2.1.1), pepsin from porcine gastric mucosa (EC 3.4.23.1), pancreatin from porcine pancreas (EC 232.468.9), bile salts and 3,5-dinitrosalicylic acid (DNS) were purchased from Sigma Aldrich (Sigma Chemical, St.Louis, USA). Other chemicals were of analytical grade. Solutions and standards were prepared using deionized water.

2.2. Chickpea starch isolation

Chickpea starch was isolated from the autochthonous chickpea (Pedrosillano variety), due to its higher content in total carbohydrates and lower fat content, compared with other cultivars (Gómez, Oliete, Rosell, Pando, & Fernández, 2008). The isolation was performed using the method described by Demirkesen-Bicak, Tacer-Caba, and Nilufer-Erdil (2018) with minor modifications. Chickpea samples were ground in a Fiztpatrick mill (Fitzmill model, Waterloo, ON, Canada). The powder was mixed with distilled water (1:10) and screened through nylon cloth (170 mesh). Sediment was successively washed with distilled water till it was free of starch. The filtrate slurry was left to rest 1 h and centrifuged at 4,000 x *g* for 5 min. The upper yellow layer was scrapped off. The white part of the sediment was resuspended in distilled water and recentrifuged for 3-4 times using the settings described above. Isolated starch was dried at 40°C for 12 h in a drying oven and stored at 4°C for further analyses.

2.3. Starch gel preparation

Starch samples were mixed with distilled water (1:10) and boiled on a water bath for 15 min, with gentle manual agitation every 2 min. Preliminary analysis were carried out to confirm the homogeneity of the gels using SEM. Gels were immersed in liquid nitrogen and kept at -80°C till freeze-drying at a pressure between 666 and 133 Pa during 24 h. Two replicates of each gel were prepared. Freeze-dried samples (average moisture content of was 14.52 ± 4.26%) were stored at 4ºC till further analysis. The absence of amylopectin retrogradation was verified using a differential scanning calorimetry analysis (data not shown).

2.4. Chemical composition of starches

Standard methods were used to determine the native starch physicochemical composition (AOAC, 2000). Total protein content was analyzed according to AOAC Method 992.23. Data were expressed as percentage on a dry weight (DW). Total starch content was determined following the AOAC Method 996.11 using a thermostable α-amylase (Termamyl®, EC 3.2.1.1) (Novozymes, Bagsværd, Denmark) and amyloglucosidase from *Rhizopus sp*. (EC 3.2.1.3) (Sigma Chemical, St.Louis, USA). Briefly, the starch sample (0.100 g ± 0.001 g) was suspended in 0.2 mL of 80% ethanol. Then, 2 mL of 1.7 M sodium hydroxide solution were added and tubes vortexed for 15 min before adding 8 mL of 600 mM sodium acetate buffer at pH 3.8. Immediately, α-amylase (280 U) and amyloglucosidase (330 U) were incorporated and samples incubated at 50°C for 30 min. An aliquot of 2 mL was centrifuged for 5 min at 10,000x *g* and the supernatant (1 mL) diluted with 10 mL of 100 mM acetate buffer at pH 5. Finally, the glucose content was measured using a glucose oxidase-peroxidase (GODPOD) kit (Megazyme International Ireland Ltd., Bray, Co. Wicklow, Ireland). The absorbance was measured using an Epoch microplate reader (Biotek Instruments,

Winooski, USA) at 510 nm. Amylose content of the starches was measured using a commercial amylose/amylopectin assay kit (K-AMYL 06/18, Megazyme International Ireland Ltd., Bray, Co. Wicklow, Ireland) based on Concanavalin A precipitation.

2.5. *In vitro* oro-gastro-intestinal digestion and reducing sugar analysis

Gel samples were subjected to successive oral, gastric and intestinal digestion following the standardized static digestion method developed by Minekus, et al. (2014) with minor modifications in the oral step. Portions of freeze-dried starch gels (1.65 g) were used for the digestion evaluation. This amount was selected considering it corresponds to the total starch ingested in 5 g of bread. To simulate oral processing during the oral phase, samples were disintegrated following the methodology described by Aleixandre, Benavent-Gil, and Rosell (2019). Starch was blended with simulated salivary fluid containing α-amylase solution (750 U) in an Ultra Turrax Tube Drive with crystal balls (IKA-Werke GmbH and Co. KG, Staufen, Germany). The gastric and intestinal digestion followed exactly the procedure previously cited (Minekus, et al., 2014). Aliquots obtained during gastric and intestinal *in vitro* digestion (200 µL) were immediately mixed with ethanol (96%) (400 µL) to stop the enzyme hydrolysis. Samples were centrifugated at 10,000 x *g* and 4°C for 5 min. The pellet was washed with ethanol (50%) (200 µL) and centrifugated again, then supernatants were pooled together. Released reducing sugars were quantified using the DNS method (Miller, 1959). Maltose content was measured in a microplate reader (Epoch Biotek Instruments, Winooski, VT, USA) at 540 nm. Experimental values were the mean of four replicates.

2.6. Starch digestion modelling

Several models (first-order kinetics, parallel and sequential kinetics) typically employed for digestion of native starches and starchy foods (Li, Dhital, Gidley, & Gilbert, 2019) were tested to fit the *in vitro* intestinal digestion of starch gels. The first-order kinetics-

based model, Eq. (1), was the most suitable to fit experimental pre-gelatinized starch digestion.

$$C = (100 - C_i - C_\infty)\exp(-k\,t) + C_\infty \qquad (1)$$

being C the fraction (%), respect to initial starch, of remnant starch to be digested at time t (min) of digestion, C_i the fraction (%) of starch hydrolyzed in the previous gastric phase ($t = 0 \rightarrow C = 100 - C_i - C_\infty + C_\infty = 100 - C_i$), k (min^{-1}) and C_∞ (%) are the kinetics constant and the fraction of undigested starch in the intestinal phase at time infinite.

The goodness of fittings was evaluated employing the coefficients of determination (r^2) and root mean square error (RMSE) Eq. (2):

$$RMSE = \sqrt{\frac{\sum_{i=1}^{N}\left(C_{exp} - C_{mod}\right)^2}{N}} \qquad (2)$$

where N is the number of experimental data and C_{exp} and C_{mod} the experimental data and calculated values by Eq. (1) of starch hydrolysis kinetics during the *in vitro* digestion.

2.7. Scanning electron microscopy (SEM)

Microstructure of starch gels, before and during digestion, were analyzed by scanning electron microscopy. Samples were coated with gold using a vacuum evaporator (JEE 400, JEOL, Tokyo, Japan). Observations were done using a SEM (SEM, S-4800, Hitachi, Ibaraki, Japan). All the images were recorded at an accelerating voltage of 10 kV.

Structure analysis of starch gels was carried out using the ImageJ software (National Institutes of Health, Bethesda, MD, USA) as reported Garzon, et al. (2020). Wall thickness (μm) and hole area (μm^2) were measured. In addition, P10, P50, and P90 were

defined to describe that 10%, 50% and 90% of the holes had a lower size or thickness than the ones indicated.

2.8. Statistical analyses

All analyses were carried out in duplicate. Mean values and standard deviations are reported. Statistical analyses of experimental results were carried out with Fisher's least significant differences test with 95% confidence. Statgraphics Centurion XV software (Statistical Graphics Corporation, Rockville, MD, USA) was used to calculate Pearson correlation coefficient (r) and P-value. Differences of $P<0.05$ were considered significant.

3. Results and discussion

3.1. Starch gels

Gels were prepared from the different starches and their microstructure was analyzed by SEM (Fig. 1). Micrographs confirmed the diverse microstructure of the different gels depending on the starch source. Gels did not show any residual starch granules, therefore, heating in water excess resulted in the complete gelatinization of the different starches. All gels displayed a honeycomb or sponge-like structure, typical pictures for gel fractures (Benavent-Gil, Román, Gómez, & Rosell, 2019). Nevertheless, visible differences were observed in the size distribution of the voids and the wall thickness. The micrographs showed that the gels obtained from cereal and tuber starches exhibited well-defined voids or holes with walls separating them. Gels from cassava and potato starches appeared like stronger networks based on the thicker walls separating the cavities. Conversely, pulses gels displayed a more irregular structure with thin and needle-like edges that resembled sub-cavities within the main network, particularly in the case of green pea gel. Li, Yeh, and Fan (2007) described a similar irregular structure

202 in gels from corn starch and soy protein concentrate composite. Because of that the
203 chemical composition of starches was assessed (Table 1).
204 All starches presented total starch contents above 90% (DW), except for wheat (89 ±
205 2.81%) and green pea (74 ± 0.5%) samples. These results were within the range of those
206 previously reported (Huang, et al., 2007; Mishra & Rai, 2006). Regarding amylose, in
207 general, cereal starches showed lower amylose levels, followed by tuber starches with
208 intermediate values and pulse starches having the highest amylose contents. Therefore,
209 amylose content varied from 14.39% in the case of rice starch to 41.05% exhibited by
210 chickpea starch. These results are in accordance with earlier reports, where pulse
211 starches showed higher amylose content than tubers and cereals (Bajaj, Singh, Kaur, &
212 Inouchi, 2018; Kaur, Shevkani, Singh, Sharma, & Kaur, 2015). The protein content of
213 cereal and tuber starches was rather low, with values ranging from 0.57 ± 0.04%
214 (cassava) to 0.89 ± 0.11% (rice). Pulse starches showed significantly higher protein
215 content, especially green pea sample (16.14 ± 0.14%). Likely, the remarkable presence
216 of proteins in those starches might explain the irregular structure above described for
217 pulse gels.
218 Image analysis was applied to evaluate the wall thickness and the area (hole size) of the
219 different holes or cavities of the gels (Fig. 2). The analysis confirmed significant
220 differences ($P < 0.001$) among the microstructure of the gels (Table 2). Regarding wall
221 thickness, despite the outliers observed, cereal-based gels showed thin walls with mean
222 values of 2.32 ± 0.84, 2.23 ± 0.81, and 2.39 ± 0.96 μm for wheat, corn, and rice,
223 respectively. Tuber and pulse gels had thicker wall cells than cereal gels, with mean
224 values ranging from 3.25 to 4.28 μm. Green pea gel exhibited bigger data dispersion,
225 which ranged from 0.83 to 9.37 μm, likely due to the sub-cavities having needle-like

walls, previously mentioned, intertwined with larger cavities. Maybe its higher protein content might also contribute to its microstructural features.

Data distribution of wall thickness and hole area of cavities was split into P10, P50 (median) and P90 to reflect the 10%, 50% and 90% of the values of those parameters lie below those percentages, respectively. The wall thickness median (P50) also showed that cereal gels had thinner walls than pulses. In the case of tubers, cassava exhibited an intermediate wall thickness median, but potato gels had an even higher median than pulses (Table 2). In addition, P90 showed that 90% of the holes exhibited very thin walls in the cereals, but the discrimination between tuber and pulses starches, previously mentioned, did not exist. The analysis of the hole area showed significant differences among starch gels ($P < 0.001$) (Table 2). All samples exhibited a right skewed distribution and several outliers. The smallest mean value area was obtained for wheat gel (654.88 μm^2), in opposition to the largest mean area obtained for rice gel (3882.15 μm^2). Also, rice gel showed the widest distribution of cavity areas.

To identify possible relationships between gels microstructure and proximate composition, correlations were evaluated. A positive correlation was observed between wall thickness P10 and the amylose content ($r = 0.76$, $P < 0.05$). This finding agrees with the reported role of amylose content in structural changes in corn starch gels, making them more resistant to swell and disintegrate (Schirmer, Höchstötter, Jekle, Arendt, & Becker, 2013). The easier interaction of linear amylose chains may cause higher integrity. Equally, a low amylose matrix, like the one obtained with rice gel, has been related to open structures that tend to disintegrate in water (Biduski, et al., 2018).

3.2. *In vitro* digestion and modelling

Gels samples were digested following an *in vitro* oro-gastrointestinal digestion, which was recorded by quantifying the reducing sugars released. Fig. 3 showed the raw starch

hydrolysis data during the oro-gastrointestinal digestion to better display the whole *in vitro* digestion.

During the oral stage, slight starch hydrolysis was detected, remaining barely constant during gastric digestion until the beginning of the intestinal phase. Previous studies reported amylase activity in the gastric phase, and they associated to some starch hydrolysis in this phase (Bustos, et al., 2017). Those authors studied the gastric digestion of different cereal-based foods, like bread, pasta, and cookies, recording starch hydrolysis during the first 60 min of the gastric phase, likely due to the residual salivary α-amylase activity. Divergences might be explained by the complexity of the food matrixes used by those authors since other polymeric compounds like the gluten network can protect salivary α-amylase in the acidic gastric medium (Bhattarai, Dhital, & Gidley, 2016). In contrast to that, the present research was performed with the unique presence of starch.

Starch hydrolysis along the different stages was evaluated following different kinetic models, but only intestinal data were further analyzed. To adjust the experimental data obtained along intestinal starch hydrolysis (Eq. 1), the mean value of the percentage of hydrolyzed starch along the gastric phase (C_i) was used (Table 3). Values for C_i ranged from 7.32% (cassava) to 18.16% (potato), indicating the significant differences in the extent of starch digestion after oral and gastric digestion, depending on the type of starch.

Starch hydrolysis during the intestinal stage was evaluated following different models and first-order kinetics model gave the best fitting (Fig. 4).

Plots showed the differences in starch hydrolysis depending on the type of starch. Wheat, corn, rice, cassava, and green pea gels showed rapid digestion in the first 120 minutes of the intestinal phase. In fact, 50% of total digestion of wheat, rice, and green

pea starches was obtained in less than 12 min (Table 3). Rice gel was digested more rapidly, during the first 0.95 min. However, a different behavior was observed for potato and chickpea gels, in which starch was not totally hydrolyzed during the 3 hours of intestine digestion, reaching a plateau (potato) at the end of the intestinal phase or even without apparent equilibrium achievement at that time (chickpea). From the kinetics model (Eq. (1)), it was possible to calculate the hydrolysis rate (k) and the percentage of undigested starch at time infinite (C_∞), and the statistical parameters for goodness assessment (Table 3).

Differences among gels could be readily evident when assessing k and C_∞. Except for rice gel, experimental data were satisfactorily fitted ($r^2 > 0.944$; $RMSE < 6.40$). Rice gel ($r^2 = 0.876$; $RMSE = 8.21$) exhibited the highest k value, suggesting a high enzymatic reaction rate. Lower amylose content starches like waxy starches show easier disruption (Schirmer, et al., 2013). Likely the weaker structure of rice gel favored the disappearance of the gel structure and the access of the enzymes to the starch gel, explaining this high digestion rate. Another atypical result was obtained with chickpea gel that had a low k value (0.013 min^{-1}) and null predicted C_∞, but digestion rate did not achieve the plateau during the 3 h. Maybe the manual isolation method used for chickpea starch can affect gel characteristics. Surely, longer experimental digestion time would allow the achievement of the plateau and a more valid C_∞ could be obtained. Previous studies stated that the digestibility of granular starches from pulses was faster than that of potato or waxy corn starches, but slower than cereal or cassava starches (Srichuwong, Sunarti, Mishima, Isono, & Hisamatsu, 2005). Present results with gels confirmed that green pea gel had faster hydrolysis than cassava, potato, wheat, and corn gels but was slower than this observed for rice gels. Nevertheless, chickpea gel showed very low digestion. In the case of granular starch from pulses, this low digestion rate has

been explained based on the high amylose content, amylose-lipid, or amylose-protein complexes (Bhattarai, et al., 2016; Chung, et al., 2008), which might also affect gels digestion, although no trend was observed considering results obtained with green pea gel. Several studies have indicated that the presence of high amylose content decreases starch digestibility due to the formation of double helices during cooling introducing an additional and relevant resistance to enzymatic action (Chung, Liu, Huang, Yin, & Li, 2010; Zhu, Liu, Wilson, Gu, & Shi, 2011). Globally, a significant negative relationship between k and amylose content (r = - 0.829) was observed in the present study, where chickpea gels (the highest amylose content) and rice gels (the lowest amylose content) showed the slowest and fastest digestion rates, respectively.

Recent studies have evaluated the effect of structural characteristics (degree of branching, molecular weight, chain lengths, etc.) of amylose and amylopectin on digestibility of native and cooked starches (Syahariza, Sar, Hasjim, Tizzotti, & Gilbert, 2013; Yu, Tao, & Gilbert, 2018). These studies suggested that the digestion rate increased with the chain length of amylose and with the low number of long amylopectin branches. To test that hypothesis with the present results, the average chain length of amylose obtained from the bibliography for the tested starches (203, 323, 300, 595, 500, 340, 1420 for wheat, corn, rice, potato, cassava, green pea and chickpea, respectively) (Bertoft, 2017; Charoenkul, Uttapap, Pathipanawat, & Takeda, 2006; Tinay, Hardalou, & Nour, 1983; Yoshimoto, Matsuda, Hanashiro, Takenouchi, & Takeda, 2001) was used to detect possible correlations. It was found an exponential (negative) relationship (r = – 0.787) between kinetics constant and amylose size, without consideration of the rice results due to its low amylose content and probable different physical and structural resistances to enzymatic activity commented above. These results suggest that the digestion rate of starch gels decreased dramatically with

increasing chain length amylose. This fact could be related to the higher recrystallization found in long-chain amylose gels (Baranowska, et al., 2020), which makes them more inaccessible to digestive enzymes.

It is important to stress that initial gel microstructure data also showed a correlation with digestion parameters (P<0.05). A highly significant positive correlation was observed for starch gel area cavities with the rate constant (r = 0.87), and for wall thickness of starch gel cavities with t50 (r = 0.81). These results suggest that bigger cavities favored the access of the digestive enzymes on the starch gels and thicker gel walls required longer to be hydrolyzed, although all intrinsic properties of gel networks might not be discarded. The latter occurred except for green pea gel, which showed the thickest cavity walls but low time for hydrolyzing 50% of the total starch. The high protein content of this gel might be responsible for the resulting wall thickness, without affecting the starch hydrolysis. Therefore, an open starch gel microstructure with big holes and thin walls is more susceptible to enzyme activity.

Trying to relate digestion results with gels microstructure, digested gels at the end of the oro-gastric and intestinal phase were microscopically observed (Fig. 5). The digested samples underwent centrifugation and freeze-drying to remove gastrointestinal fluids. In the present study, gels kept their structure after the oral phase, except for the cereal gels that lost much of their structures (Fig. 5, column 1). Baudron, Gurikov, Smirnova, and Whitehouse (2019) reported that freeze-drying conditions might affect the density and surface area of the starch gels. Even when this methodology may affect starch gel structures, micrographs confirmed different digestion performance of the gels, depending on the starch origin. In tubers and pulses gels, the honeycomb structure remained in a certain way after oral digestion. After gastric phase, potato micrographs (Fig. 5, D2) showed a plane surface with small cavities. Likely, the faster potato

hydrolysis indicated by C_i, led to the removal of the fragile parts of the structure, only remaining the compact one with small cavities. Plane structures with small holes are less accessible to intestinal digestive enzymes, hindering starch digestibility, which would explain the lower kinetic constant (k) obtained in the intestinal phase. Conversely, cassava gels revealed a more open structure at the end of gastric digestion, being easier the diffusion of enzymes trough starch and digestion fragments. In spite of the low starch hydrolysis of starch gels in the gastric phase, other factors like the acidic pH might explain changes in the gel structure. Great structural changes were observed in the pulse gels after the gastric phase, although starch was barely hydrolyzed. Those changes might be linked to the protease activity of the pepsin added in the stomach phase, which hydrolyze the protein fraction of those gels changing their structure. At the end of the intestinal digestion, in the cereal starches the initial structure was completely lost. Potato and chickpea samples kept the typical structure of starch gels in some way (Fig. 5, D3, and G3). This observation agrees with digestion results, where potato and chickpea starch gels did not achieve the digestion equilibrium. However, also cassava gel (Fig. 5, E3) maintained some cavities, but the digestion results showed total starch hydrolysis at 120 min. Probably, digestive enzymes attack the more accessible parts of this gel, keeping the porous structure.

4. Conclusions

This study showed significant differences in the structure of starch gels from different sources, particularly, in the gel cavities areas and the thickness of the hole walls. Cereal based gels showed thinner walls, compared to tuber and pulses starches. Some microstructural features with thin and needle-like edges of starch gels from pulses were associated to high protein content. Regarding the area of the cavities, tuber, and pulses gels showed bigger cavities, although rice gel gave the biggest hole area. Starch gel

hydrolysis through a standardized oro-gastrointestinal *in vitro* digestion was different for each starch gel, and microscope analyses revealed changes in gel structure from the beginning of *in vitro* digestion. The fitting method was applied to analyze the kinetics of the intestinal stage, and the first-order kinetics model reproduced satisfactorily the starch hydrolysis trend during intestinal *in vitro* digestion, except for rice starch. Differences in starch digestibility were observed depending on the starch source. It was confirmed that the amylose content of starch gels played an important role in their hydrolysis. However, the initial microstructure of gels showed a correlation with digestion parameters, where bigger cavities facilitated the starch hydrolysis.

Author Contributions: Credit roles: AA: Conceptualization; Data curation; Formal analysis; Investigation; Methodology; Roles/Writing - original draft; YBG: Methodology; Supervision; RM: Formal analysis; Writing - review & editing; Funding acquisition; CMR: Conceptualization; Funding acquisition; Investigation; Supervision; Data curation; Writing - review & editing.

Declaration of interest: none

Acknowledgments

Authors acknowledge the financial support of the Spanish Ministry of Science and Innovation (Project RTI2018-095919-B-C2) and the European Regional Development Fund (FEDER) and Generalitat Valenciana (Project Prometeo 2017/189).

References

Aleixandre, A., Benavent-Gil, Y., & Rosell, M. C. (2019). Effect of Bread Structure and In Vitro Oral Processing Methods in Bolus Disintegration and Glycemic Index. *Nutrients, 11*(9).

AOAC. (2000). *Official methods of analysis of the AOAC International*: Association of Analytical Communities.

Bajaj, R., Singh, N., Kaur, A., & Inouchi, N. (2018). Structural, morphological, functional and digestibility properties of starches from cereals, tubers and legumes: a comparative study. *Journal of Food Science and Technology*, *55*(9), 3799-3808.

Baranowska, H. M., Sikora, M., Krystyjan, M., Dobosz, A., Tomasik, P., Walkowiak, K., Masewicz, Ł., & Borczak, B. (2020). Analysis of the Retrogradation Processes in Potato Starches Blended with Non-Starchy Polysaccharide Hydrocolloids by LF NMR. *Food Biophysics, 15*(1), 64-71.

Baudron, V., Gurikov, P., Smirnova, I., & Whitehouse, S. (2019). Porous Starch Materials via Supercritical- and Freeze-Drying. *Gels (Basel, Switzerland), 5*(1), 12.

Benavent-Gil, Y., Román, L., Gómez, M., & Rosell, C. M. (2019). Physicochemical Properties of Gels Obtained from Corn Porous Starches with Different Levels of Porosity. *Starch - Stärke, 71*(3-4), 1800171.

Bertoft, E. (2017). Understanding Starch Structure: Recent Progress. *Agronomy, 7*(3), 56.

Bhattarai, R. R., Dhital, S., & Gidley, M. J. (2016). Interactions among macronutrients in wheat flour determine their enzymic susceptibility. *Food Hydrocolloids, 61*, 415-425.

Biduski, B., Silva, W., Colussi, R., Halal, S., Lim, L.-T., Dias, Á., & Zavareze, E. (2018). Starch hydrogels: The influence of the amylose content and gelatinization method. *International Journal of Biological Macromolecules, 113*, 443-449.

Brodkorb, A., Egger, L., Alminger, M., Alvito, P., Assunção, R., Ballance, S., Bohn, T., Bourlieu-Lacanal, C., Boutrou, R., Carrière, F., Clemente, A., Corredig, M., Dupont, D., Dufour, C., Edwards, C., Golding, M., Karakaya, S., Kirkhus, B., Le Feunteun, S., Lesmes, U., Macierzanka, A., Mackie, A. R., Martins, C., Marze, S., McClements, D. J., Ménard, O., Minekus, M., Portmann, R., Santos, C. N., Souchon, I., Singh, R. P., Vegarud, G. E., Wickham, M. S. J., Weitschies, W., & Recio, I. (2019). INFOGEST static in vitro simulation of gastrointestinal food digestion. *Nature Protocols, 14*(4), 991-1014.

Bustos, M. C., Vignola, M. B., Pérez, G. T., & León, A. E. (2017). In vitro digestion kinetics and bioaccessibility of starch in cereal food products. *Journal of Cereal Science, 77*, 243-250.

Butterworth, P. J., Warren, F. J., Grassby, T., Patel, H., & Ellis, P. R. (2012). Analysis of starch amylolysis using plots for first-order kinetics. *Carbohydrate Polymers, 87*(3), 2189-2197.

Chambers, E. S., Byrne, C. S., & Frost, G. (2019). Carbohydrate and human health: is it all about quality? *The Lancet, 393*(10170), 384-386.

Charoenkul, N., Uttapap, D., Pathipanawat, W., & Takeda, Y. (2006). Molecular Structure of Starches from Cassava Varieties having Different Cooked Root Textures. *Starch - Stärke, 58*(9), 443-452.

Chung, H.-J., Lim, H. S., & Lim, S. T. (2006). Effect of partial gelatinization and retrogradation on the enzymatic digestion of waxy rice starch. *Journal of Cereal Science, 43*(3), 353-359.

Chung, H.-J., Liu, Q., Donner, E., Hoover, R., Warkentin, T. D., & Vandenberg, B. (2008). Composition, molecular structure, properties, and in vitro digestibility of starches from newly released Canadian pulse cultivars. *Cereal Chemistry, 85*(4), 471-479.

Chung, H.-J., Liu, Q., Huang, R., Yin, Y., & Li, A. (2010). Physicochemical Properties and In Vitro Starch Digestibility of Cooked Rice from Commercially Available Cultivars in Canada. In *Cereal Chemistry* (Vol. 87, pp. 297-304): John Wiley & Sons, Ltd.

Demirkesen-Bicak, H., Tacer-Caba, Z., & Nilufer-Erdil, D. (2018). Pullulanase treatments to increase resistant starch content of black chickpea (Cicer arietinum L.) starch and the effects on starch properties. *International Journal of Biological Macromolecules, 111*, 505-513.

Feltre, G., Almeida, F. S., Sato, A. C. K., Dacanal, G. C., & Hubinger, M. D. (2020). Alginate and corn starch mixed gels: Effect of gelatinization and amylose content on the properties and in vitro digestibility. *Food Research International, 132*, 109069.

Frei, M., Siddhuraju, P., & Becker, K. (2003). Studies on the in vitro starch digestibility and the glycemic index of six different indigenous rice cultivars from the Philippines. *Food Chemistry, 83*(3), 395-402.

Garzon, R., & Rosell, C. M. (2020). Rapid assessment of starch pasting using a rapid force analyzer. *Cereal Chemistry, n/a*(n/a).

Gómez, M., Oliete, B., Rosell, C. M., Pando, V., & Fernández, E. (2008). Studies on cake quality made of wheat–chickpea flour blends. *LWT - Food Science and Technology*, *41*(9), 1701-1709.

Goñi, I., Garcia-Alonso, A., & Saura-Calixto, F. (1997). A starch hydrolysis procedure to estimate glycemic index. *Nutrition Research, 17*(3), 427-437.

Huang, J., Schols, H. A., van Soest, J. J. G., Jin, Z., Sulmann, E., & Voragen, A. G. J. (2007). Physicochemical properties and amylopectin chain profiles of cowpea, chickpea and yellow pea starches. *Food Chemistry, 101*(4), 1338-1345.

Jayakody, L., & Hoover, R. (2008). Effect of annealing on the molecular structure and physicochemical properties of starches from different botanical origins – A review. *Carbohydrate Polymers, 74*(3), 691-703.

Kaur, A., Shevkani, K., Singh, N., Sharma, P., & Kaur, S. (2015). Effect of guar gum and xanthan gum on pasting and noodle-making properties of potato, corn and mung bean starches. *Journal of Food Science and Technology, 52*(12), 8113-8121.

Lavoisier, A., & Aguilera, J. M. (2019). Effect of a Whey Protein Network Formed by Cold Gelation on Starch Digestibility. *Food Biophysics, 14*(2), 214-224.

Li, Dhital, S., Gidley, M. J., & Gilbert, R. G. (2019). A more general approach to fitting digestion kinetics of starch in food. *Carbohydrate Polymers, 225*, 115244.

Li, Yeh, A.-I., & Fan, K.-L. (2007). Gelation characteristics and morphology of corn starch/soy protein concentrate composites during heating. *Journal of Food Engineering, 78*(4), 1240-1247.

Lineback, D. R., & Wongsrikasem, E. (1980). Gelatinization of starch in baked products. *Journal of Food Science, 45*(1), 71-74.

Martinez, M. M. (2020). Starch Nutritional Quality: Beyond Intraluminal Digestion in Response to Current Trends. *Current Opinion in Food Science, n/a*(n/a).

Miller, G. (1959). Use of Dinitrosalicylic Acid Reagent for Determination of Reducing Sugar. *Analytical Chemistry, 31*, 426-428.

Minekus, M., Alminger, M., Alvito, P., Ballance, S., Bohn, T., Bourlieu, C., Carrière, F., Boutrou, R., Corredig, M., Dupont, D., Dufour, C., Egger, L., Golding, M., Karakaya, S., Kirkhus, B., Le Feunteun, S., Lesmes, U., Macierzanka, A., Mackie, A., Marze, S., McClements, D. J., Ménard, O., Recio, I., Santos, C. N., Singh, R. P., Vegarud, G. E., Wickham, M. S. J., Weitschies, W., & Brodkorb, A. (2014). A standardised static in vitro digestion method suitable for food – an international consensus. *Food & Function, 5*(6), 1113-1124.

Mishra, S., & Rai, T. (2006). Morphology and functional properties of corn, potato and tapioca starches. *Food Hydrocolloids, 20*(5), 557-566.

Noda, T., Takigawa, S., Matsuura-Endo, C., Suzuki, T., Hashimoto, N., Kottearachchi, N. S., Yamauchi, H., & Zaidul, I. S. M. (2008). Factors affecting the digestibility of raw and gelatinized potato starches. *Food Chemistry, 110*(2), 465-470.

Schirmer, M., Höchstötter, A., Jekle, M., Arendt, E., & Becker, T. (2013). Physicochemical and morphological characterization of different starches with variable amylose/amylopectin ratio. *Food Hydrocolloids, 32*(1), 52-63.

Segura, M. E. M., & Rosell, C. M. (2011). Chemical composition and starch digestibility of different gluten-free breads. *Plant Foods for Human Nutrition, 66*(3), 224.

Srichuwong, S., Sunarti, T. C., Mishima, T., Isono, N., & Hisamatsu, M. (2005). Starches from different botanical sources I: Contribution of amylopectin fine structure to thermal properties and enzyme digestibility. *Carbohydrate Polymers, 60*(4), 529-538.

Syahariza, Z. A., Sar, S., Hasjim, J., Tizzotti, M. J., & Gilbert, R. G. (2013). The importance of amylose and amylopectin fine structures for starch digestibility in cooked rice grains. *Food Chemistry, 136*(2), 742-749.

Tinay, A. H. E., Hardalou, S. B. E., & Nour, A. M. (1983). Comparative study of three legume starches. *International Journal of Food Science & Technology, 18*(1), 1-9.

Yoshimoto, Y., Matsuda, M., Hanashiro, I., Takenouchi, T., & Takeda, Y. (2001). Molecular structure and pasting properties of legume starches. *Journal of Applied Glycoscience, 48*(4), 317-324.

Yu, W., Tao, K., & Gilbert, R. G. (2018). Improved methodology for analyzing relations between starch digestion kinetics and molecular structure. *Food Chemistry, 264*, 284-292.

Zhang, Ao, Z., & Hamaker, B. R. (2006). Slow Digestion Property of Native Cereal Starches. *Biomacromolecules, 7*(11), 3252-3258.

Zhu, L.-J., Liu, Q.-Q., Wilson, J. D., Gu, M.-H., & Shi, Y.-C. (2011). Digestibility and physicochemical properties of rice (Oryza sativa L.) flours and starches differing in amylose content. *Carbohydrate Polymers, 86*(4), 1751-1759.

Table 1. Chemical composition of starches from different sources (%, DW)

Starch source	Protein	Total starch	Amylose
Wheat	0.64 ± 0.08^{a}	88.94 ± 2.81^{b}	27.64 ± 0.25^{b}
Corn	0.88 ± 0.02^{b}	94.70 ± 2.06^{c}	28.13 ± 2.48^{b}
Rice	0.89 ± 0.11^{b}	95.63 ± 2.06^{c}	14.39 ± 0.07^{a}
Potato	0.58 ± 0.01^{a}	92.90 ± 0.65^{bc}	29.38 ± 1.14^{bc}
Cassava	0.57 ± 0.04^{a}	92.32 ± 2.49^{bc}	32.09 ± 0.72^{c}
Green pea	16.14 ± 0.14^{d}	74.24 ± 0.50^{a}	38.49 ± 1.81^{d}
Chickpea	1.78 ± 0.02^{c}	91.62 ± 1.54^{bc}	41.05 ± 0.67^{d}

Means within a column followed with different letters are significantly different ($P<0.05$).

Table 2. Microstructure characteristics of starch gels from different sources

Starch source	Wall thickness (μm)				Hole area (μm^2)			
	Mean ± SD	P10	P50	P90	Mean ± SD	P10	P50	P90
Wheat	2.32 ± 0.84^{a}	1.35	2.32	3.55	654.88 ± 452.89^{a}	212.60	436.71	1298.85
Corn	2.23 ± 0.81^{a}	1.42	2.16	2.95	874.93 ± 756.07^{ab}	194.20	550.63	2101.60
Rice	2.39 ± 0.96^{a}	1.41	2.24	3.36	3882.15 ± 1981.35^{e}	1431.74	3729.66	6635.78
Potato	4.28 ± 2.20^{d}	2.00	3.82	6.49	1956.68 ± 1360.75^{d}	689.22	1647.08	3912.44
Cassava	3.25 ± 1.26^{b}	1.89	2.89	5.42	1418.11 ± 1644.03^{c}	356.23	810.66	2725.76
Green pea	4.06 ± 2.03^{cd}	1.99	3.49	7.21	1284.60 ± 981.65^{bc}	434.85	891.30	2823.56
Chickpea	3.71 ± 1.43^{bc}	2.32	3.57	5.43	1449.34 ± 1120.67^{c}	450.20	1048.42	2754.92
P-value	0.0000				0.0000			

P10, P50 (median), and P90 indicates that 10%, 50% or 90% of the values (wall thickness or hole area) lie to the ones specified.

Table 3. Statistical parameters for goodness assessment of non-linear fitting with a first-order kinetics-based model (Eq. (1))

Starch source	C_i (%)	k (min^{-1})	C_∞ (%)	r^2	*RMSE*	t50 (min)*
Wheat	14.42	0.061	0.00	0.978	5.76	5.7
Corn	15.03	0.039	0.00	0.975	6.40	11.8
Rice	10.37	0.265	0.00	0.876	8.21	0.95
Potato	18.16	0.024	27.70	0.944	5.79	36.5
Cassava	7.32	0.043	0.00	0.987	4.75	14.4
Green pea	9.01	0.064	14.10	0.959	6.27	9.3
Chickpea	7.82	0.013	0.00	0.990	3.85	45.0

*t50, digestion time to reach the 50% of the total starch digestion

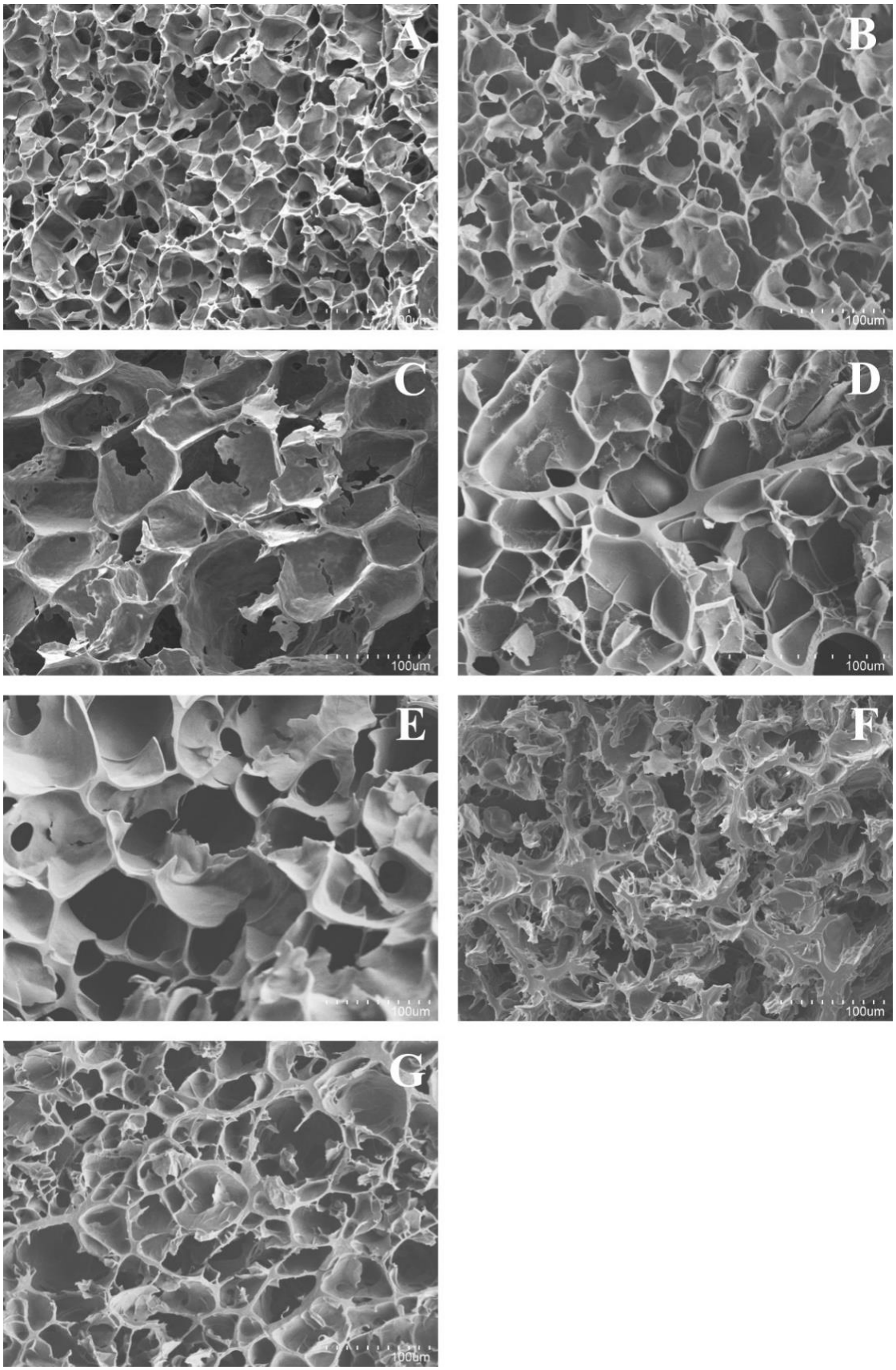

542

543 **Fig. 1.** SEM micrographs of starch gels from wheat (A), corn (B), rice (C), potato (D),

544 cassava (E), green pea (F), chickpea (G). Magnification x300.

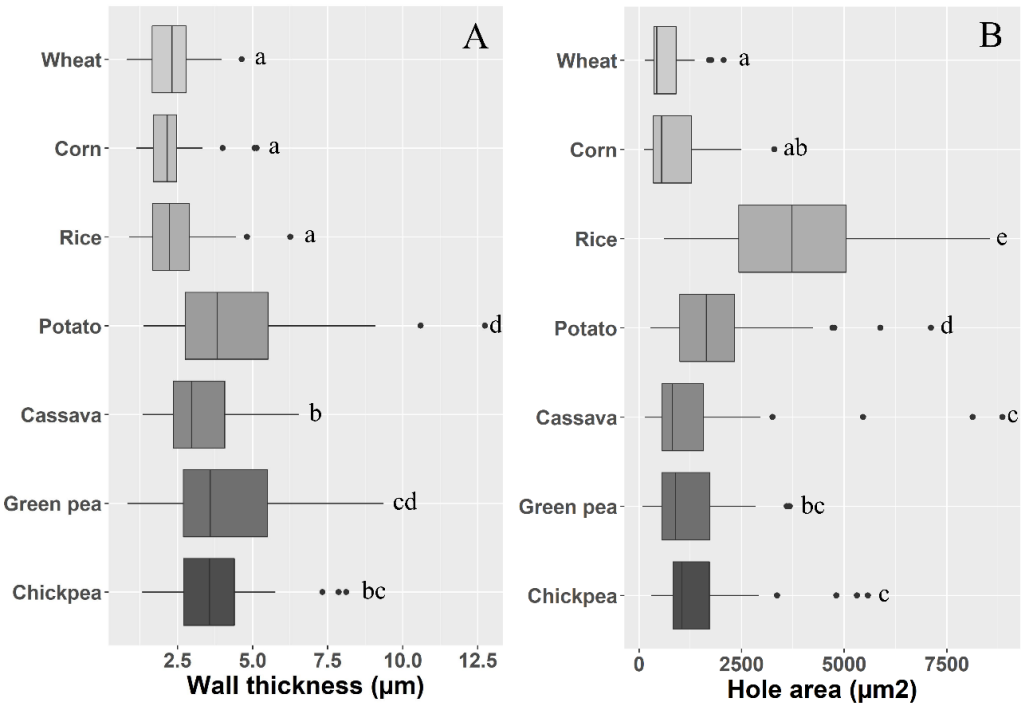

545

546 **Fig. 2.** Boxplots showing the parameters calculated by image analysis of the gel
547 micrographs. A) Wall thickness and B) hole size distribution.
548

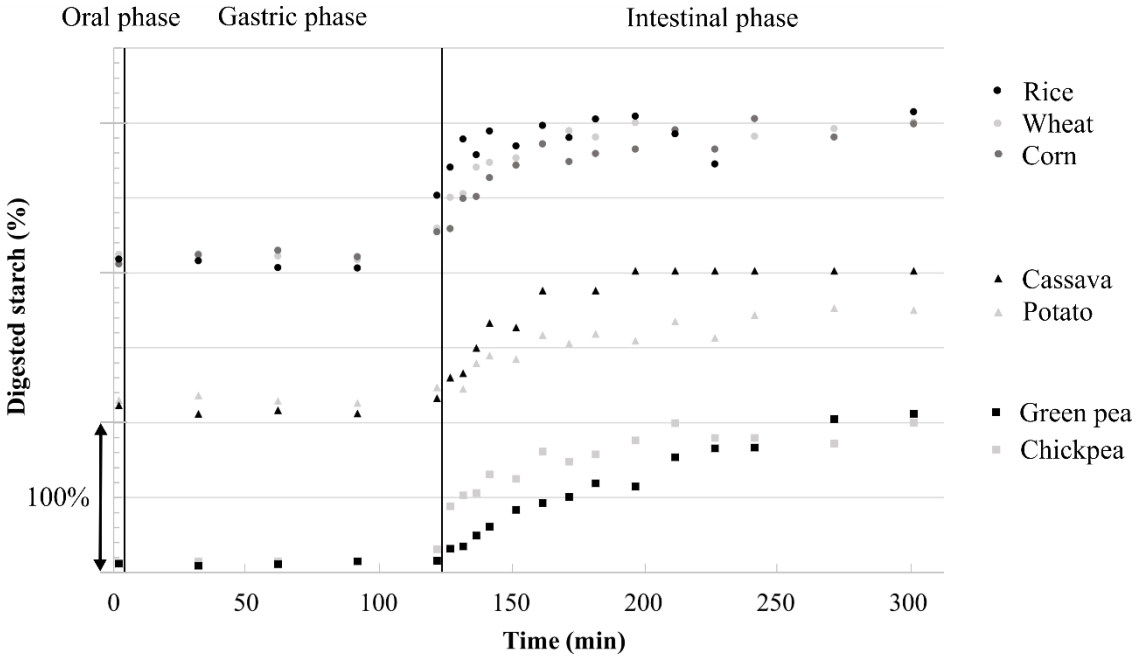

Fig. 3. Starch hydrolysis from starch gels during the oro-gastrointestinal *in vitro* digestion. Vertical lines divided the graph into digestion phases: oral, gastric, and intestinal. Starch gels were grouped according to their source proximity. Scale bar of 100% indicates the value of the graduation marks.

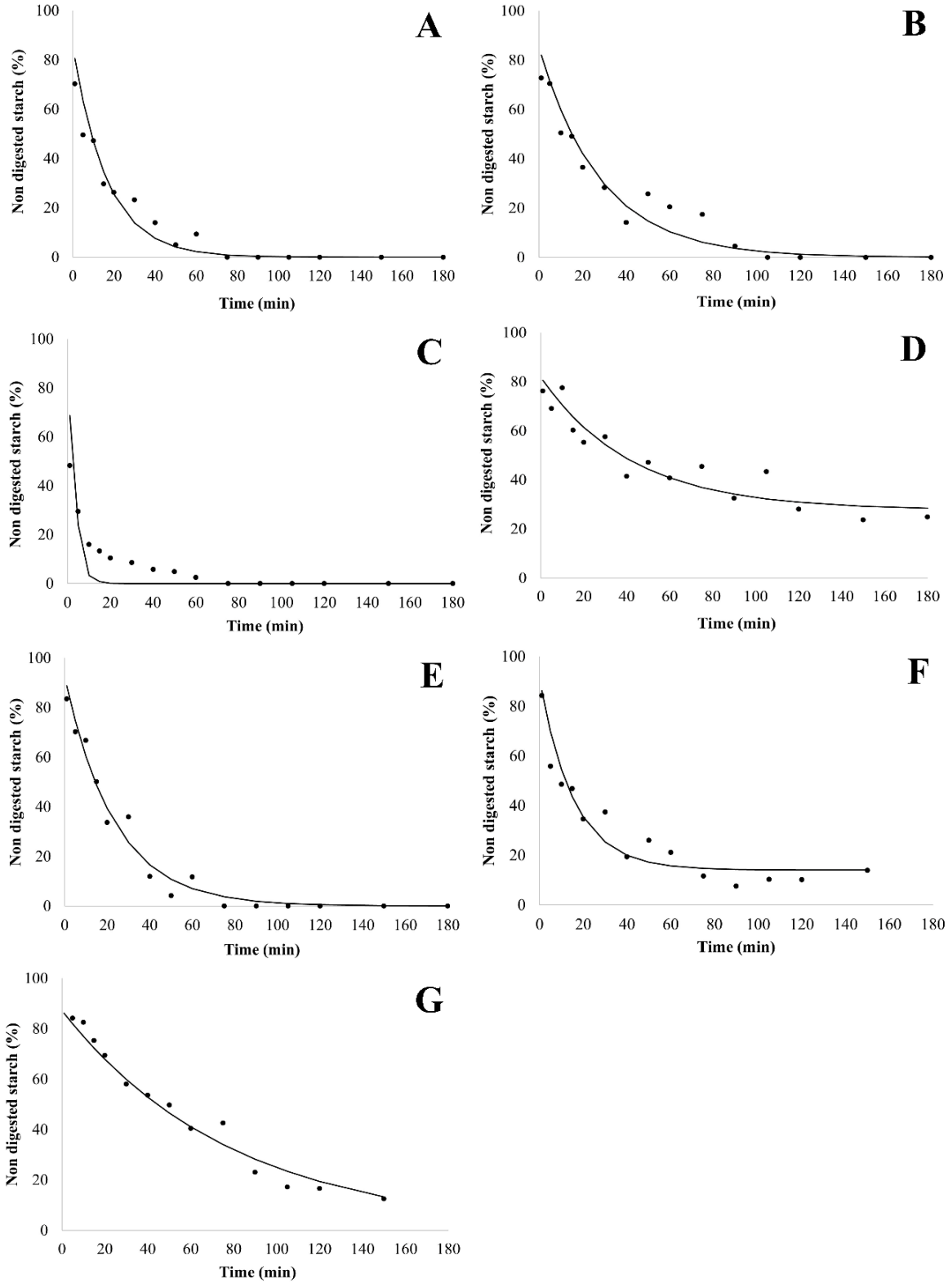

Fig. 4. Starch digestibility plots during intestinal *in vitro* digestion for wheat (A), corn (B), rice (C), potato (D), cassava (E), green pea (F), chickpea (G) gels.

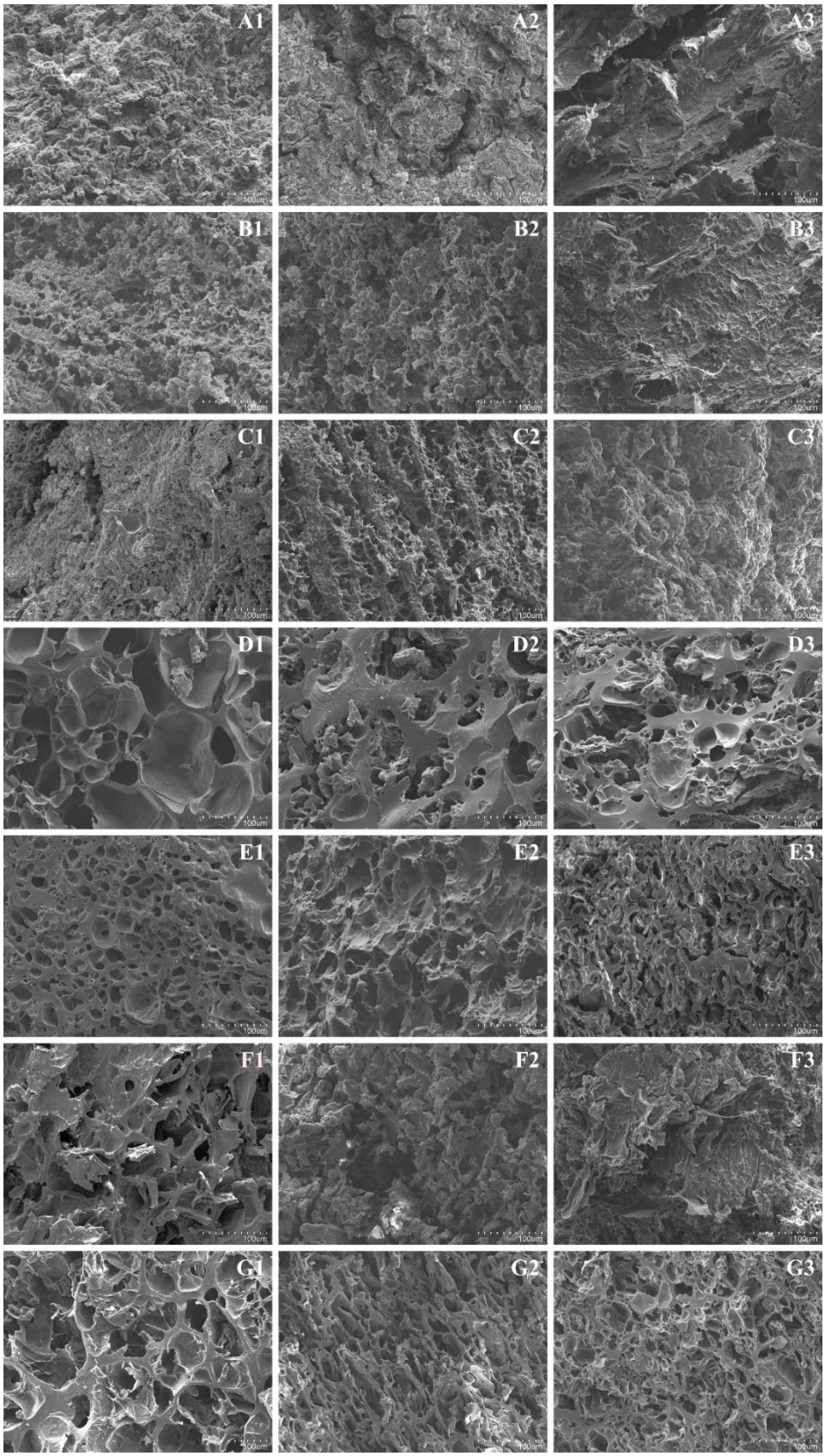

Fig. 5. SEM micrographs of digested starch gels after oral (1), gastric (2) and intestinal (3) *in vitro* digestion. Gels were obtained from wheat (A), corn (B), rice (C), potato (D), cassava (E), green pea (F), chickpea (G). Magnification x300.